JOURNAL OF SOLID STATE CHEMISTRY 62, 317–327 (1986)

Luminescence and Energy Transfer in a Highly Symmetrical System: $Eu_2Ti_2O_7$

P. A. M. BERDOWSKI AND G. BLASSE

Physics Laboratory, Solid State Department, Utrecht University, P.O. Box 80.000, 3508 TA Utrecht, The Netherlands

Received August 19, 1985

Luminescence and energy transfer properties of $Gd_2Ti_2O_7$:Eu and $Eu_2Ti_2O_7$ are reported. Transfer between unperturbed (intrinsic) Eu^{3+} ions and perturbed (extrinsic) Eu^{3+} ions has been observed. At low temperatures the emission spectra of $Eu_2Ti_2O_7$ are dominated by trap emission, due to direct energy transfer from the intrinsic Eu^{3+} ions to the extrinsic Eu^{3+} ions. Above 10 K energy migration among the Eu^{3+} ions to quenching centers occurs. The interaction between the Eu^{3+} ions is probably exchange in character. The nature of the extrinsic Eu^{3+} ions has been elucidated.

1. Introduction

In the course of our investigations on two-dimensional, concentrated Eu^{3+} systems, we recently reported on the energy migration properties of $NaEuTiO_4$ (*1*), $Eu_2O_2SO_4$ (*2*), and EuOCl (*3*). It was shown that for these compounds concentration quenching occurs down to 1.2 K. The decay characteristics of the Eu^{3+} emission point to anisotropic energy migration among the Eu^{3+} ions to quenching centers. The anisotropic energy migration behavior can be explained by the fact that the Eu^{3+} ions form double layers perpendicular to the *c* axis in these compounds. The nearest-neighbor distance between Eu^{3+} ions in the layers is approximately the same for the three systems, viz. 3.7 Å.

Although energy migration among the Eu^{3+} ions has been observed down to 1.2 K, we were not able to elucidate the character of the Eu^{3+}–Eu^{3+} energy transfer interaction. The theory for the energy transfer process was initially developed by Förster (*4*) and later extended by Dexter (*5*). For the case of multipolar coupling the energy transfer probability depends on the probability of the multipolar transitions on the ions involved. For Eu^{3+} at low temperatures the only resonant transition giving rise to energy transfer is $^5D_0 \leftrightarrows {}^7F_0$. The strongly forbidden nature of this transition explains the fact that no energy migration among Eu^{3+} ions can be observed in several concentrated Eu^{3+} systems at low temperatures [see, e.g., Refs. (*6, 7*)].

There are two possible explanations for the observation of energy migration at low temperatures in the three compounds mentioned above. It is known that in some compounds the $^5D_0 \leftrightarrows {}^7F_0$ transition is not strictly forbidden (*8–11*). This can be explained by the presence of a linear crystal field at the europium site in these compounds (*12, 13*). Since in these three com-

0022-4596/86 $3.00

pounds the Eu^{3+} ions are incorporated on sites with a linear crystal field, the $^5D_0 \leftrightarrows {}^7F_0$ selection rule is lifted, and energy transfer between Eu^{3+} ions via multipole–multipole interaction may be expected. However, another explanation for the observation of energy migration at low temperatures is, that due to the relatively small distance between the Eu^{3+} ions, energy transfer occurs via exchange interaction.

The aim of the present investigation is to study the energy migration behavior in a concentrated Eu^{3+} compound, in which the Eu^{3+} ion occupies a lattice site with a center of symmetry, and in which the nearest-neighbor distance between Eu^{3+} ions is again ~3.7 Å. In this case all electric-dipole transitions are forbidden, so that energy transfer between Eu^{3+} ions via multipole–multipole interaction is impossible at low temperatures. Such systems can contribute to the knowledge about the energy transfer interaction between Eu^{3+} ions with a short separation.

We investigated the luminescence and energy transfer properties of $Gd_{1.98}Eu_{0.02}Ti_2O_7$ and $Eu_2Ti_2O_7$ in which only one crystallographic site is available for Eu^{3+}. The site symmetry is D_{3d}, i.e., the Eu^{3+} ions are on a center of symmetry. The nearest-neighbor distance between the Eu^{3+} ions in $Eu_2Ti_2O_7$ is ~3.6 Å. The luminescence properties of $Gd_2Ti_2O_7$: Eu were described in Refs. (*14*, *15*). The luminescence properties of the concentrated compound have not been reported.

$Eu_2Ti_2O_7$ represents a family of compounds isostructural to the mineral pyrochlore, $(Na,Ca)_2(Nb,Ta)_2O_6(F,OH)$. The crystal structure of rare-earth pyrochlores has been investigated by several authors (*17*, *19*), and can be described in several different ways. Knop (*17*) described it as a network structure of corner linked TiO_6 octahedra with the rare-earth ions filling the interstices. Aleshin (*20*) described it on basis of an anion-deficient fluorite unit cell, while Sleight (*21*) described it as interpenetrating networks of TiO_6 octahedra and RE_2O' chains, where O′ indicates the oxygen ions which are coordinated to the rare-earth ions only. It has been shown that the former is more stable and forms the "backbone" of the structure (*22*). The RE^{3+} ions are eight-coordinated and are at the center of a puckered hexagonal ring (chair form) of six O^{2-} ions. Normal to the mean plane of this hexagon is a pair of O′ ions. This results in a site symmetry D_{3d} for the RE ions. Figure 1 shows the crystal structure of $Eu_2Ti_2O_7$.

2. Experimental

All measurements described below were performed on powdered samples. The compounds were prepared in two different ways. On the one hand, they were prepared by firing intimate mixtures of Gd_2O_3, Eu_2O_3, and TiO_2 for several periods (6 hr at 1050°C, 10 hr at 1200°C, and 2 hr at 1450°C). On the other hand, they were prepared by dissolving the rare-earth oxides and TiO_2 in

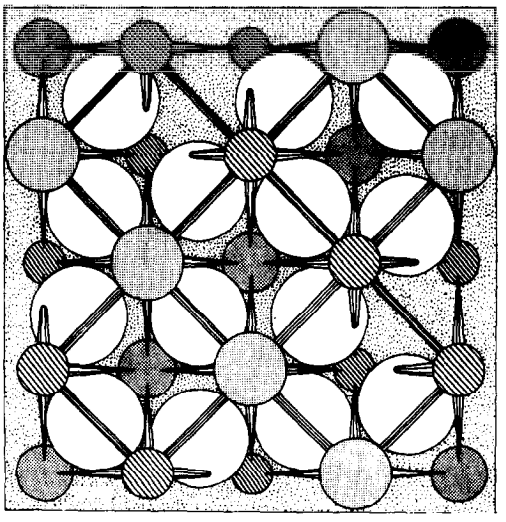

FIG. 1. Crystal structure of europium titanate ($Eu_2Ti_2O_7$). Open circles, O^{2-}; hatched circles, Ti^{4+}; dotted circles, Eu^{3+}.

HCl. By adding concentrated ammonia the hydroxides were precipitated. The resulting powder was fired in air in a quartz ampulla at 400°C for 5 hr and at 900°C for 1 hr. Finally, it was fired under O_2 atmosphere (3×10^3 Torr) for 4 hr at 1000°C. The resulting products had a white color, and were checked by X-ray powder diffraction using Cu$K\alpha$ radiation. The diffuse reflection spectra were recorded using a Perkin–Elmer UV/VIS spectrophotometer (Lambda 7). The setup for the other optical measurements has been described in Refs. (*1*, *2*).

3. Results

3.1. Spectral Properties

The excitation spectrum of the Eu^{3+} emission of $Gd_{1.98}Eu_{0.02}Ti_2O_7$ consists of lines and a broad band with a maximum at 300 nm. In the excitation spectrum of the Eu^{3+} emission of $Eu_2Ti_2O_7$ two broad bands can be distinguished with maxima at 300 and 320 nm. At low Eu^{3+} concentrations the band corresponds to the absorption of the exciting radiation by the TiO_6 groups followed by energy transfer to Eu^{3+}. In the concentrated compounds the charge-transfer band of the Eu^{3+} ion can be observed separately (*1*, *23*).

Due to the center of symmetry at the Eu^{3+} site all electric-dipole transitions are strictly forbidden, and only the magnetic dipole transition $^5D_0 \rightarrow {}^7F_1$ is expected in the emission spectrum of $Gd_{1.98}Eu_{0.02}Ti_2O_7$. The emission spectra of $Gd_{1.98}Eu_{0.02}Ti_2O_7$ after excitation into the $^5D_1$ level at 18,977.5 cm^{-1} show two main peaks in the $^5D_0 \rightarrow {}^7F_1$ spectral region. The magnetic dipole transition $^5D_0 \rightarrow {}^7F_1$ is split, since the $^7F_1$ level splits into a singlet and a doublet under D_{3d} symmetry. In addition to the peaks corresponding to the $^5D_0 \rightarrow {}^7F_1$ transition, weak peaks can be observed in the region where the $^5D_0 \rightarrow {}^7F_2$ emission is to be expected. The appearance of these peaks was also reported in Ref. (*14*), where they were assigned to vibronic transitions. However, their intensity increases for decreasing temperatures. Also in the $^5D_0 \rightarrow {}^7F_1$ spectral region weak peaks can be observed in the vicinity of the main peaks. This is illustrated in Fig. 2, which shows the emission spectrum of $Gd_{1.98}Eu_{0.02}Ti_2O_7$ after selective excitation into the $^5D_1$ level at 18,977.5 cm^{-1}, recorded at 4.2 K in the $^5D_0 \rightarrow {}^7F_1$ spectral region. The presence of these so-called satellite peaks suggest that there are different types of sites for the Eu^{3+} ions.

In order to obtain information on the differently surrounded Eu^{3+} ions we recorded the excitation spectra for the $^5D_0 \rightarrow {}^7F_1$ main emission line (589.3 nm) and a satellite line (593.8 nm) of $Gd_{1.98}Eu_{0.02}Ti_2O_7$ in the $^7F_0 \rightarrow {}^5D_1$ spectral region at 4.2 K (see Fig. 3). The excitation spectrum of the main line at 589.3 nm consists of two sharp lines at

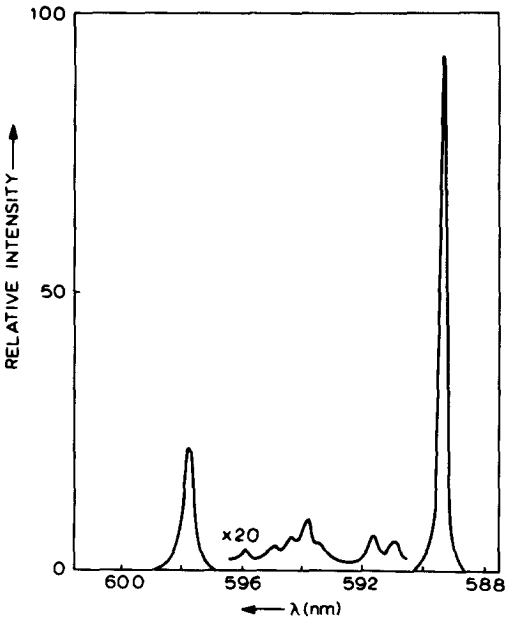

FIG. 2. Emission spectrum of $Gd_{1.98}Eu_{0.02}Ti_2O_7$ upon excitation into the $^5D_1$ level (at 18,977.5 cm^{-1}) of the Eu^{3+} ions, recorded at 4.2 K in the $^5D_0 \rightarrow {}^7F_1$ spectral region.

518.8 (not shown in Fig. 3a) and 526.9 nm, corresponding to the $^7F_0 \rightarrow {}^5D_1$ transition on the unperturbed (intrinsic) Eu^{3+} ions, and a weak line at 526.4 nm, which is probably due to a small amount of second phase. The linewidth of the main peak at 526.9 nm is 2 cm^{-1}. The excitation spectrum of the satellite line at 593.8 nm shows the same main lines, but also various satellite lines (see Fig. 3b). The broadening of the lines is due to a lower resolution of the optical equipment because of the low intensity of the emission. The occurrence of the main excitation peaks at 518.8 and 526.9 nm seems to point to energy transfer from the intrinsic Eu^{3+} ions to the perturbed (extrinsic) Eu^{3+} ions. Since the $^7F_0 \rightarrow {}^5D_1$ transition can at the utmost split into three lines, the number of lines observed in the $^7F_0 \rightarrow {}^5D_1$ region (eleven) points to at least four different sites for the Eu^{3+} ions.

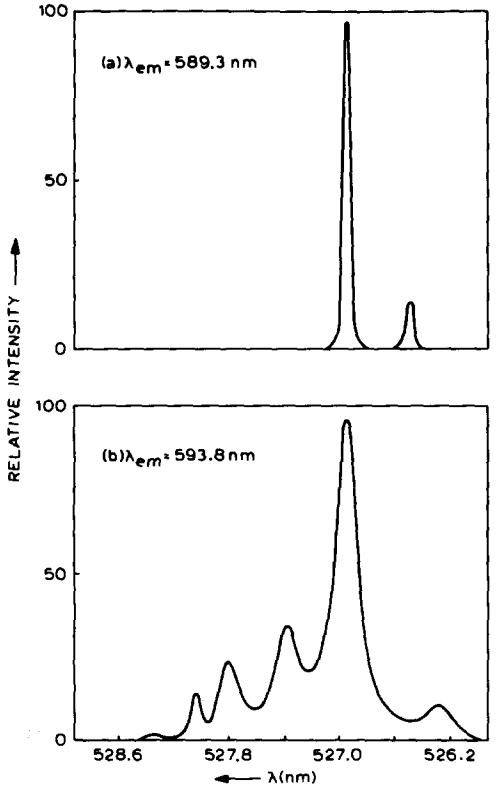

FIG. 3. Excitation spectra of the emission of $Gd_{1.98}Eu_{0.02}Ti_2O_7$, recorded at 4.2 K in the $^7F_0 \rightarrow {}^5D_1$ spectral region. (a) Emission wavelength 589.3 nm; (b) emission wavelength 593.8 nm.

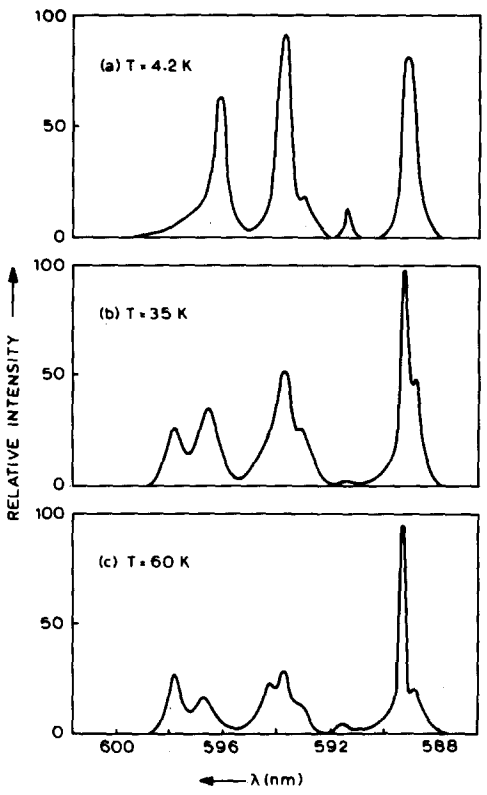

FIG. 4. Emission spectra of $Gd_{1.98}Eu_{0.02}Ti_2O_7$ in the $^5D_0 \rightarrow {}^7F_1$ spectral region at various temperatures. Excitation is into the $^5D_1$ level of extrinsic Eu^{3+} ions (527.8 nm).

We used a tunable dye laser to excite selectivity the extrinsic Eu^{3+} ions with the $^7F_0 \rightarrow {}^5D_1$ peak at 527.8 nm. Figure 4a shows the emission spectrum in the $^5D_0 \rightarrow {}^7F_1$ spectral region recorded at 4.2 K. It is clear that the number of peaks as well as their positions differ from those in Fig. 2. The peaks corresponding to the intrinsic emission at 589.3 and 597.8 nm cannot be distinguished. With increasing temperatures the shape of the emission spectrum changes, which is illustrated in Figs. 4b and c. At 60 K the intrinsic emission dominates,

which is probably due to thermally activated energy transfer from the extrinsic Eu^{3+} ions to the intrinsic Eu^{3+} ions.

Due to the low absorption strength of the $^7F_J \rightarrow {}^5D_{J'}$ transitions, the recorded diffuse reflection spectrum of $Gd_{1.98}Eu_{0.02}Ti_2O_7$ does not allow reliable interpretation. Figure 5 shows the diffuse reflection spectrum of $Eu_2Ti_2O_7$, recorded at 300 K. The two main peaks in the $^7F_0 \rightarrow {}^5D_1$ spectral region at 527 and 519 nm correspond to the $^7F_0 \rightarrow {}^5D_1$ transition on the intrinsic Eu^{3+} ions. The three peaks indicated by arrows coincide with the excitation lines of the extrinsic emission (see above) and are therefore ascribed to absorption by the extrinsic ions. If an equal absorption strength is assumed for the $^7F_0 \rightarrow {}^5D_1$ transitions of the Eu^{3+} ions at different sites, the concentration of extrinsic ions can be estimated from the diffuse reflection spectrum. This assumption is not unreasonable, since we are dealing with a magnetic-dipole transition, of which the probability is expected to vary only slightly with the variation of surroundings. From the diffuse reflection spectrum we obtained an estimate of ~4 mole% (i.e., 6×10^{20} cm^{-3}) for the concentration of extrinsic ions.

The emission spectra of $Eu_2Ti_2O_7$ after excitation into the $^5D_1$ level of the intrinsic Eu^{3+} ions, recorded at low temperatures, are dominated by emission from extrinsic Eu^{3+} ions. Emission peaks can be observed in the $^5D_0 \rightarrow {}^7F_0$, $^5D_0 \rightarrow {}^7F_1$, and $^5D_0 \rightarrow {}^7F_2$ spectral regions. The domination by extrinsic emission is illustrated in Fig. 6a, which shows the emission spectrum in the $^5D_0 \rightarrow {}^7F_1$ spectral region, recorded at 1.2 K. The hatched peak at 589.6 nm corresponds to the $^5D_0 \rightarrow {}^7F_1$ transition on the intrinsic Eu^{3+} ions. The emission spectra show a strong temperature dependence, which is illustrated in Figs. 6b and c. Above ~35 K the emission spectra consist mainly of the peaks corresponding to the $^5D_0 \rightarrow {}^7F_1$ transition on the intrinsic Eu^{3+} ions. At 1.2 K the concentrated samples give a bright luminescence. Above 10 K the intensity of the luminescence decreases rapidly. At room temperature the intensity of the luminescence of the concentrated samples is less than that of the diluted one, indicating strong, temperature-dependent concentra-

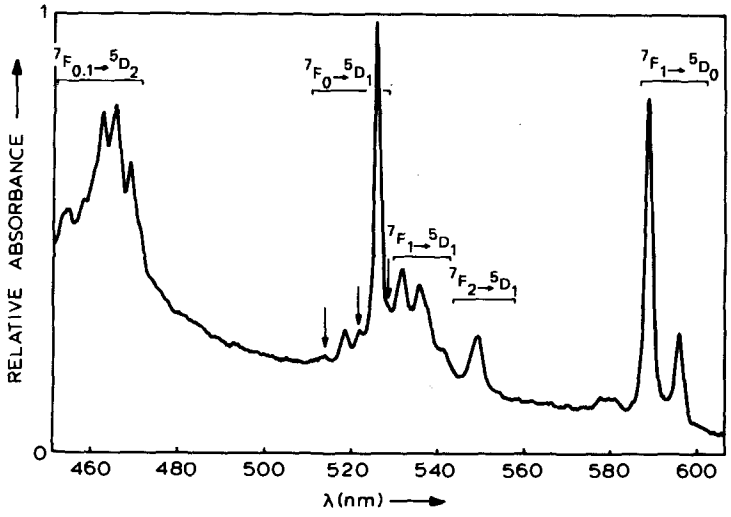

FIG. 5. Diffuse reflection spectrum of $Eu_2Ti_2O_7$ recorded at 300 K.

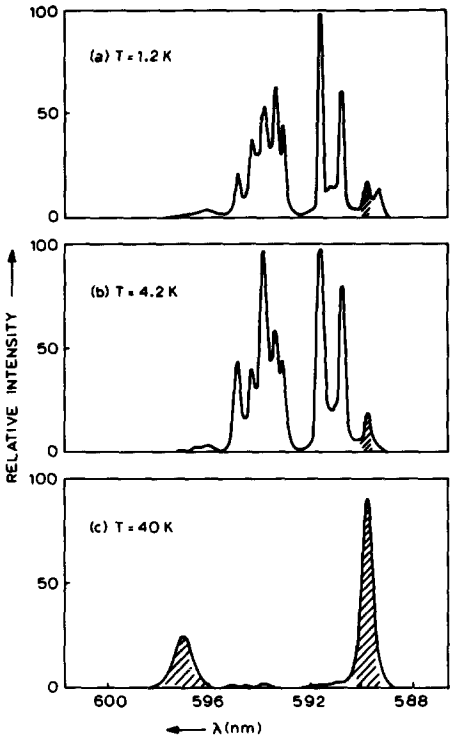

FIG. 6. Emission spectra of $Eu_2Ti_2O_7$ in the $^5D_0 \rightarrow {}^7F_1$ spectral region at various temperatures. The peaks corresponding to the emission from intrinsic Eu^{3+} ions are hatched.

tion quenching of the luminescence. The quenching behavior above 10 K accounts for the broadening of the lines in Fig. 6c, which is due to a lower resolution of the optical equipment. Apparently the extrinsic ions trap the excitation energy at low temperatures. The traps are emptied at higher temperatures, whereupon the emission is quenched.

Figure 7a shows the excitation spectrum of the intrinsic $^5D_0 \rightarrow {}^7F_1$ emission at 589.6 nm, in the $^7F_0 \rightarrow {}^5D_1$ spectral region at 1.2 K. In addition to the intrinsic excitation peak at 526.9 nm, other peaks can be distinguished in the excitation spectrum. The occurrence of the relatively intense peaks in the region 526.5 to 526.8 nm is probably due to the overlap of the intrinsic and extrinsic emission peaks (see Fig. 6a). However, the increase of the relative intensity of the peaks in the region 527 to 530 nm with increasing temperature (see Fig. 7b) suggests thermally activated energy transfer from extrinsic Eu^{3+} ions to intrinsic Eu^{3+} ions, similar to the diluted system (see Fig. 4). Figure 7c shows the excitation spectrum of the main extrinsic emission peak at 591.5 nm, recorded at 4.2 K.

3.2. Time Dependence of the Luminescence

The decay characteristics of the $^5D_0$ emission were investigated as a function of temperature both for $Gd_{1.98}Eu_{0.02}Ti_2O_7$ and $Eu_2Ti_2O_7$. For the diluted system the decay curves of the intrinsic emission after excita-

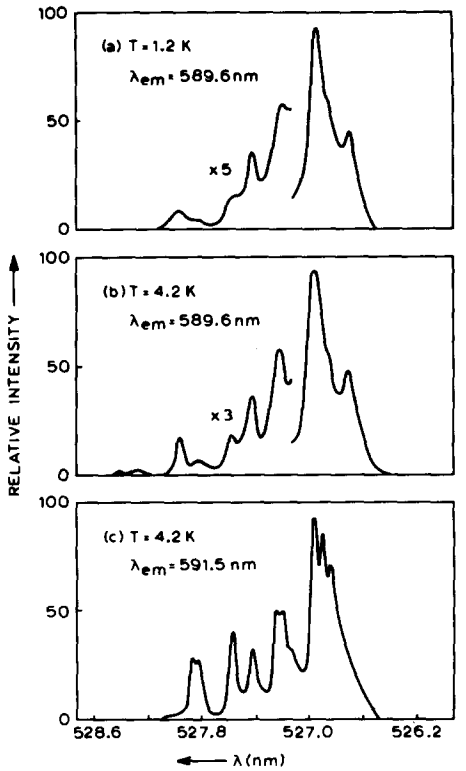

FIG. 7. Excitation spectra of the emission of $Eu_2Ti_2O_7$ recorded in the $^7F_0 \rightarrow {}^5D_1$ spectral region (a) at 1.2 K for emission wavelength 589.6 nm; (b) at 4.2 K for emission wavelength 589.6 nm; (c) at 4.2 K for emission wavelength 591.5 nm.

tion into the $^5D_1$ level of the intrinsic Eu^{3+} ions show an initially nonexponential part, followed by an exponential tail, with a temperature-independent decay rate of 247 sec^{-1}. Under the same excitation conditions the decay curve of the extrinsic emission at 593.8 nm, recorded at 4.2 K, shows a buildup, eventually followed by an exponential tail. The decay rate derived from this exponential part is 521 sec^{-1}. The decay rate increases and the buildup becomes faster with increasing temperature. The increasing decay rate is ascribed to back-transfer from extrinsic Eu^{3+} ions (see above). Figures 8 and 9 show the decay curves of the intrinsic emission of $Eu_2Ti_2O_7$ after excitation into the $^5D_1$ level of the intrinsic Eu^{3+} ions, at various temperatures. At low temperatures the decay curves of the intrinsic emission consist of an initially nonexponential part, followed by an exponential tail (see Fig. 8). The decay rate of the exponential part was 800 sec^{-1} at 1.2 K. With increasing temperature a faster decay is observed in the initial part (see Fig. 9). The contribution of the exponential part increases up to ~7.5 K, above which it decreases rapidly.

The decay curves of the emission from the $^5D_0$ level of the extrinsic Eu^{3+} ions upon excitation into the $^5D_1$ level of the intrinsic

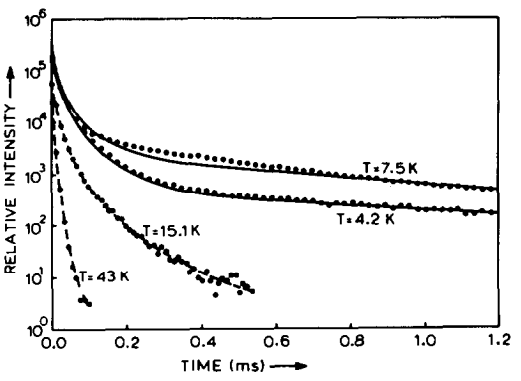

FIG. 9. Decay curves of the intrinsic Eu^{3+} emission (589.6 nm) in $Eu_2Ti_2O_7$ at various temperatures (exc. 526.9 nm). The drawn and broken curves present fits to different models as discussed in the text.

Eu^{3+} ions in $Eu_2Ti_2O_7$ show a temperature dependent buildup. This effect is illustrated in Fig. 10, which shows the decay curves of the extrinsic emission at 4.2 and 7.5 K. Above 10 K the buildup could not be observed under the experimental conditions applied. The tail of the decay curves could be approximated by a single-exponential up to ~5 K. The decay rate obtained from the decay curve recorded at 1.2 K is 770 sec^{-1}. The decay curves presented in Fig. 10 give the most convincing demonstration that energy transfer from the intrinsic Eu^{3+} ions to the extrinsic ones occurs.

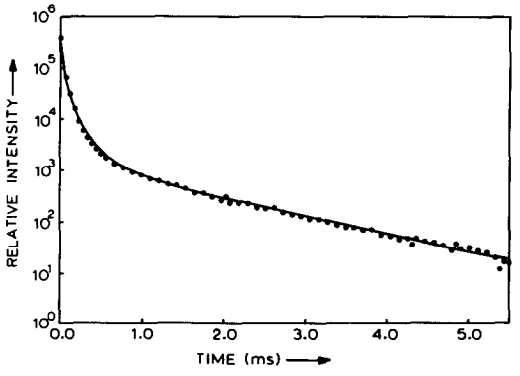

FIG. 8. Decay curve of the intrinsic Eu^{3+} emission (589.6 nm) in $Eu_2Ti_2O_7$ recorded at 1.2 K (exc. 526.9 nm). Drawn curve presents fit discussed in the text.

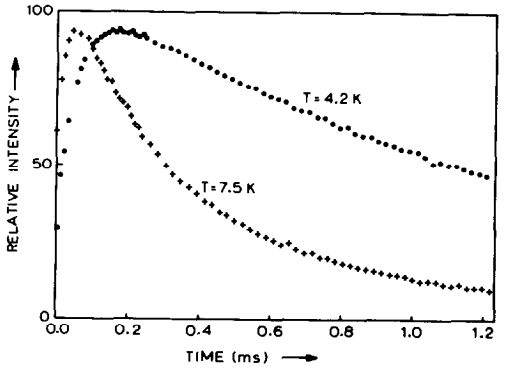

FIG. 10. Decay curves of the extrinsic Eu^{3+} emission (591.5 nm) after excitation into the $^5D_1$ level of the intrinsic Eu^{3+} ions (exc. 526.9 nm) at 4.2 and 7.5 K.

4. Discussion

From the measurements on the diluted as well as on the concentrated compounds it is clear that emission from Eu^{3+} ions on different types of sites occurs. Though the emission from extrinsic Eu^{3+} ions is only very weak in the emission spectra of $Gd_{1.98}Eu_{0.02}Ti_2O_7$, it dominates the emission spectra of $Eu_2Ti_2O_7$ at low temperatures. The existence of different types of sites for Eu^{3+} in pyrochlore compounds has been investigated by Faucher and Caro (*24*). It was shown that emission from differently surrounded Eu^{3+} ions could be observed in the emission spectrum of $Eu_2Zr_2O_7$. No emission spectra of $Eu_2Ti_2O_7$ were presented, which is probably due to the strong concentration quenching which has been reported to occur in most concentrated pyrochlore rare-earth titanates (*25*). The occurrence of different sites for the Eu^{3+} ions in zirconates was ascribed to anion disorder, which is consistent with the observation of anomalously broad lines in the Raman spectra (*26*). The presence of different lattice sites for rare-earth ions in pyrochlore titanates has also been reported for $Gd_2Ti_2O_7:Nd^{3+}$ (*27*).

We recorded Raman spectra for $Gd_{1.98}Eu_{0.02}Ti_2O_7$ and $Eu_2Ti_2O_7$, and observed broad lines ($\Delta_{1/2} \sim 65\ cm^{-1}$), comparable to those observed for the zirconates. Since no anomalous behavior was observed in the X-ray spectra of our compounds, this points to anion disorder in the compounds under study. The two different methods of synthesis lead to the same results. The existence of a seizable amount of anion disorder can be explained by the fact that in a pyrochlore unit cell there are eight (a) sites and eight (b) sites for eight O′ ions. In the ideal pyrochlore structure all O′ ions are incorporated on the (a) sites (see Fig. 1). The observation of anion disorder is probably due to the occupation of (b) sites by O′ ions. This would result in vacancies on the (a) sites by which the symmetry of neighboring Eu^{3+} ions is lowered from D_{3d} to C_{3v}. This explains the observation of the $^5D_0 \rightarrow {}^7F_0$ emission in the spectra of $Eu_2Ti_2O_7$, since this transition is not strictly forbidden for C_{3v} symmetry (*12, 13*). An anion vacancy will also affect the surroundings of next-nearest-neighbor Eu^{3+} ions, so that different types of extrinsic Eu^{3+} ions can be expected. Also the O′ ions on (b) sites will result in the presence of perturbed Eu^{3+} ions.

Transition metal ions are potential impurities in titanium oxide. Some of these ions are well-known quenchers of the Eu^{3+} emission, as might be the case for $Eu_2Ti_2O_7$. Another possible quenching center could be Eu^{2+}.

From the luminescence spectra of $Gd_{1.98}Eu_{0.02}Ti_2O_7$ it is clear that energy transfer between the intrinsic Eu^{3+} ions and the extrinsic Eu^{3+} ions occurs. The shape of the decay curves of the emission from the intrinsic and the extrinsic Eu^{3+} ions after excitation into the $^5D_1$ level of the former can be explained in terms of this transfer. The initial part of the decay curves of the intrinsic emission recorded at low temperatures could be approximated by an $\exp(-at^{1/2})$ dependence, which is expected for the case of direct energy transfer without back-transfer (*28*). The direct transfer model predicts an exponential tail with a decay rate equal to the radiative rate. Below, we assume the radiative decay rate of the intrinsic Eu^{3+} emission in $Gd_2Ti_2O_7:Eu$ equal to the decay rate derived from the exponential tail of the decay curves of the intrinsic Eu^{3+} emission of $Gd_{1.98}Eu_{0.02}Ti_2O_7$ ($247\ sec^{-1}$).

The effect of energy transfer from the intrinsic Eu^{3+} ions to the extrinsic Eu^{3+} ions is obviously more drastic in $Eu_2Ti_2O_7$ than in $Gd_{1.98}Eu_{0.02}Ti_2O_7$. As stated above, the decay curves of the intrinsic Eu^{3+} emission in $Eu_2Ti_2O_7$ recorded at low temperatures approached also a single-exponential a long

time after the pulse. Since the exponential tails of the decay curves correspond to a decay rate which is much faster than the radiative rate of the intrinsic emission, direct transfer to extrinsic ions can be ruled out as the only transfer mechanism. If we assume energy migration among the intrinsic Eu^{3+} ions, the shape of the decay curves of the intrinsic Eu^{3+} emission in $Eu_2Ti_2O_7$ recorded at low temperatures suggests diffusion-limited energy migration (*29–32*). However, the decay curves recorded at these temperatures could not be fitted satisfactorily to the theoretical expressions.

A comparable decay behavior has been observed for the intrinsic Tb^{3+} emission in TbF_3 at low temperatures, where trap emission dominates also the emission spectra (*33*). The observed exponential tail for the decay curves of the intrinsic Tb^{3+} emission in TbF_3 was shown to arise from thermally activated back-transfer from the extrinsic Tb^{3+} ions to the intrinsic ones. If the exponential component of the decay curves of the intrinsic Eu^{3+} emission in $Eu_2Ti_2O_7$ is due to the same process, this would account for the stronger contribution of this component at 7.5 K, compared to the decay curve recorded at 4.2 K. However, an initial exponential decay was observed for the decay of the intrinsic Tb^{3+} emission in Tb^{3+} at low temperatures, which is explained by rapid energy migration among the intrinsic Tb^{3+} ions (*33*). Apparently, due to the relatively high concentration of extrinsic ions in $Eu_2Ti_2O_7$ compared to that in TbF_3 (6×10^{20} vs 1.2×10^{19} cm^{-3}), direct transfer to extrinsic ions dominates the initial part of the decay curve of the intrinsic Eu^{3+} emission in $Eu_2Ti_2O_7$. If we assume that the exponential tail of the decay curves recorded at low temperatures is due to back-transfer from the extrinsic ions, the decay rate obtained from this tail should correspond to the decay rate of the extrinsic emission at these temperatures. The comparable decay rates obtained from the decay curves of the intrinsic and extrinsic emission recorded at low temperatures supports this assumption. For this reason we tried to fit the decay curves of the intrinsic Eu^{3+} emission in $Eu_2Ti_2O_7$ to the following expression

$$I(t) = A\exp(-p_{int}t - Bt^{1/2}) + C\exp(-p_{ext}t), \quad (1)$$

where $I(t)$ is the emission intensity at time t, p_{int} the radiative decay rate of the intrinsic Eu^{3+} ions (247 sec^{-1}), and p_{ext} the summation of the extrinsic radiative decay rate and the back-transfer rate. It should be stated that overlap of intrinsic and extrinsic emission peaks also will contribute to the second term of Eq. (1). The drawn curves in Figs. 8 and 9 represent the best fits according to Eq. (1).

The discrepancy between the theoretical fit and the experimental data in the initial part of the decay curve recorded at 1.2 K could be due to another type of interaction between the intrinsic Eu^{3+} ions and the extrinsic Eu^{3+} ions than the dipole–dipole interaction assumed in Eq. (1). The only type of interaction giving rise to a faster decay would be exchange interaction (*28*), which is most likely in view of the strictly forbidden $^5D_0 \rightarrow {}^7F_0$ transition on the intrinsic Eu^{3+} ions.

The fit for the decay curve recorded at 7.5 K is less satisfactory. This is probably due to the fact that other extrinsic Eu^{3+} ions with a lower trap depth will empty at this temperature (see also Fig. 10).

The initial part of the decay curves recorded above ~10 K could not be fitted to Eq. (1). As stated above, the onset of the luminescence quenching is also at ~10 K. This leads us to the conclusion that above 10 K the excitation energy migrates over the Eu^{3+} sublattice to quenching centers. Therefore, we tried to fit the decay curves recorded above 10 K to the well-known expression derived by Yokota and Tanimoto (*29*):

$$I(t) = I(0)\exp(-p_{int}t) \exp\left[-4/3\pi^{3/2}N_a(Ct)^{1/2}\left(\frac{1 + 10.87x + 15.50x^2}{1 + 8.743x}\right)^{3/4}\right], \quad (2)$$

where $x = DC^{-1/3}t^{2/3}$, N_a is the quencher concentration, C the coupling constant for the europium–quencher interaction, and D the diffusion constant. N_a, C, and D were introduced as fitting parameters. The broken curves in Fig. 9 represent the best fits according to Eq. (2), and were obtained with $N_a = 1.2 \times 10^{20}$ cm^{-3}, $C = 1 \times 10^{-37}$ cm^6 sec^{-1}, and $D = 9 \times 10^{-12}$ cm^2 sec^{-1} for the decay curve recorded at 15.1 K, and $N_a = 2 \times 10^{19}$ cm^{-3}, $C = 5 \times 10^{-35}$ cm^6 sec^{-1}, and $D = 3 \times 10^{-9}$ cm^2 sec^{-1} for the decay curve recorded at 43 K. The relatively high values of N_a obtained from the fit to the experimental data recorded at 15.1 K is probably due to the fact that at 15.1 K a considerable amount of migrating excitation energy is trapped by extrinsic ions. The obtained values for C and D are comparable to those found for C and D in similar systems [see Ref. (*3*)].

In conclusion, we have evaluated the luminescence and energy transfer properties of $Gd_2Ti_2O_7$:Eu and $Eu_2Ti_2O_7$. The luminescence spectra of the concentrated compounds are dominated by emission from extrinsic Eu^{3+} ions, present due to a considerable degree of anion disorder. At low temperatures the excited intrinsic Eu^{3+} ions transfer directly to the extrinsic ones, where the excitation energy is trapped. With increasing temperature the extrinsic Eu^{3+} traps empty, whereupon the excitation energy can migrate through the Eu^{3+} sublattice. The observations suggest that energy transfer between the Eu^{3+} ions occurs via exchange interaction. By studying the interaction in pairs of RE^{3+} ions, Vial and Buisson have shown that the mechanism of superexchange is effective if the distances between the RE^{3+} ions are short (*35, 36*). The efficiency of this mechanism was already observed for $GdCl_3$, $Gd(OH)_3$, and $Tb(OH)_3$ from exciton dispersion measurements (*37, 38*).

Acknowledgments

The authors are indebted to Mrs. J. van Keulen and G. J. Dirksen for the preparation of the samples. The investigations were supported by the Netherlands Foundation for Chemical Research (SON) with financial aid from the Netherlands Organization for Advancement of Pure Research (ZWO).

References

1. P. A. M. Berdowski and G. Blasse, *J. Lumin.* **29,** 243 (1984).
2. P. A. M. Berdowski, R. van Mens, and G. Blasse, *J. Lumin.* **33,** 147 (1985).
3. P. A. M. Berdowski, J. van Herk, and G. Blasse, *J. Lumin.* **34,** 9 (1985).
4. T. Förster, *Ann. Phys.* **2,** 55 (1948).
5. D. L. Dexter, *J. Chem. Phys.* **21,** 836 (1953).
6. M. J. Weber, *Phys. Rev. B: Condens. Matter* **4,** 2932 (1971).
7. F. Kellendonk and G. Blasse, *J. Chem. Phys.* **75,** 561 (1981).
8. Z. J. Kiss and H. A. Weakliem, *Phys. Rev. Lett.* **15,** 457 (1965).
9. W. C. Nieuwpoort and G. Blasse, *Solid State Commun.* **4,** 379 (1966).
10. B. G. Wybourne, *J. Chem. Phys.* **48,** 2596 (1968).
11. R. D. Peacock, *Struct. Bonding* **22,** 83 (1975).
12. B. R. Judd, *Phys. Rev.* **127,** 750 (1962).
13. B. R. Judd, *J. Chem. Phys.* **44,** 839 (1966).
14. G. Blasse, A. Bril, and W. C. Nieuwpoort, *J. Phys. Chem. Solids* **27,** 1587 (1966).
15. R. A. McCauley and F. A. Hummel, *J. Lumin.* **6,** 105 (1973).
16. R. S. Roth, *J. Res. Nat. Bur. Stand.* **56,** 17 (1956).
17. O. Knop, F. Brisse, L. Castelliz, and Sutarno, *Canad. J. Chem.* **43,** 2812 (1965).
18. O. Knop, F. Brisse, and L. Castelliz, *Canad. J. Chem.* **47,** 971 (1969).
19. W. J. Becker and G. Will, *Z. Kristallogr.* **131,** 278 (1970).
20. E. Aleshin and R. Roy, *J. Amer. Ceram. Soc.* **45,** 18 (1962).
21. A. W. Sleight, *Inorg. Chem.* **7,** 1704 (1968); **8,** 2039 (1969).
22. J. Pannetier, *J. Phys. Chem. Solids* **34,** 583 (1973).

23. G. BLASSE AND A. BRIL, *J. Chem. Phys.* **48,** 3652 (1968).
24. M. FAUCHER AND P. CARO, *J. Solid State Chem.* **12,** 1 (1975).
25. L. H. BRIXNER, *Inorg. Chem.* **3,** 1065 (1964).
26. O. MICHEL, M. PEREZ Y JORBA, AND R. COLLONGUES, *Mater. Res. Bull.* **9,** 1457 (1974).
27. V. A. ANTONOV, P. A. ARSENEV, AND D. S. PETROVA, *Phys. Status Solidi A* **41,** K127 (1977).
28. M. INOKUTI AND F. HIRAYAMA, *J. Chem. Phys.* **43,** 1978 (1965).
29. M. YOKOTA AND O. TANIMOTO, *J. Phys. Soc. Japan* **22,** 779 (1967).
30. A. I. BURSHTEIN, *Sov. Phys. JETP (Engl. Transl.)* **35,** 882 (1972).
31. D. L. HUBER, *Phys. Rev.* **20,** 2307 (1979).
32. K. K. GOSH AND D. L. HUBER, *J. Lumin.* **21,** 225 (1980).
33. M. F. JOUBERT, B. JACQUIER, R. MONCORGÉ, AND G. BOULON, *J. Phys. (Paris)* **43,** 893 (1982).
34. M. F. JOUBERT, B. JACQUIER, AND R. MONCORGÉ, *Phys. Rev. B: Condens. Matter* **28,** 3725 (1983).
35. J. C. VIAL AND R. BUISSON, *J. Phys. Lett.* **43,** L745 (1982).
36. R. BUISSON, private communication.
37. R. S. MELTZER AND H. W. MOOS, *Phys. Rev. B: Condens. Matter* **6,** 264 (1972).
38. R. L. CONE AND R. S. MELTZER, *J. Chem. Phys.* **62,** 3573 (1975).